Chapter 31

Rare and Forbidden Charm Decays[1]

31.1 Introduction

The smashingly successful Standard Model of particle physics describes matter's most basic elements and the forces through which they interact. Physicists have tested its predictions to better than 1% precision. Yet despite its many successes, we know the SM is not the whole story. The questions of so-called fine-tuning, mass hierarchy and so on are remained unexplained. Testing the SM is one of the most important mission in particle physics. One most important feature of the SM is the absence of FCNC at tree level. Generally FCNC processes begin at one loop level and GIM suppressed, which have been proved to be powerful tools for probing the structure of electro-weak interactions. Examples are rare K and B decays and oscillations induced by penguin or box Feynman diagrams. Due to the large mass of top quark, the GIM suppression is mild for down-type quarks. As for charm quark FCNC processes, only down type quarks could propagate in the loop, so that the GIM suppression is very strong and the SM predictions are very tiny, which would be beyond the sensitivities of any running or planned colliders. So that such decays would be sensitive probes of New Physics beyond the SM. However, the long distance contribution could be much larger than the SM short distance effects, which are not always reliably calculable. These decays include: (i) $D \to V\gamma(V = \rho, \omega, \phi, ...)$, (ii)$D \to X\ell^+\ell^-$ $(X = \pi, K, \eta, \rho, \omega, \phi, ...)$, (iii) $D \to X\nu_\ell\bar{\nu}_\ell$ $(X = \pi, K, \eta, \ldots)$, (iv) $D \to \gamma\gamma$, (v) $D \to \ell^+\ell^-$.

Theoretically, there are lots of works which have been intended to calculate both short and long distance contributions in these decays as reliably as possible in the SM and consider possible new physics scenarios with potentially large effects. In many cases, extensions of the SM could give contributions sometimes orders or magnitude larger than the SM [291]. In order to establish the existence of a clean window for observation of new physics in a given observable in rare charm decays, the SM contributions should be made clear at first. This is very important to include the long distance contributions due to the propagation of light quarks, although they are hard to be calculated with analytical methods. In what following, we will first review these decays in the SM and then in new physics models.

[1]By Hai-Bo Li and Ya-Dong Yang

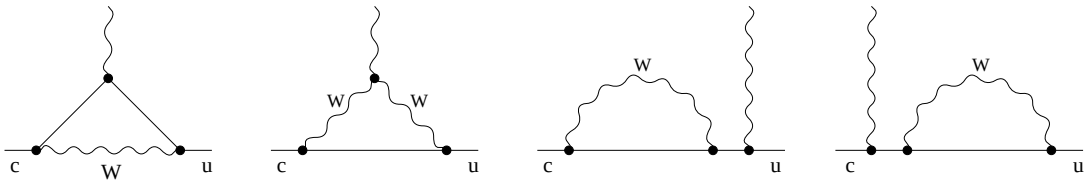

Figure 31.1: One-loop diagrams inducing the $c \to u\gamma$

31.2 The rare charm decays in the SM

In principle, the task of producing SM predictions for FCNC D meson decays is straightforward. There are two components to the analysis, short-distance (SD) and long-distance (LD), which must be separately calculated. It is known that the SD contribution can be calculated with well defined framework, but phenomenological methods have to be resorted for LD contributions.

31.2.1 Radiative charm decays

The radiative decay modes with one photon include $D \to V\gamma$, $D_s \to V\gamma$ and $D \to X_u\gamma$. The short distance effective Hamiltonian for $c \to u + \gamma$ starts from one loop diagrams as shown in Fig.1 which give

$$L_{int} = -\frac{4G_F}{\sqrt{2}}\, A\, \frac{e}{16\pi^2}\, m_c(\bar{u}\sigma_{\mu\nu}P_R c)F^{\mu\nu}, \tag{31.1}$$

with

$$\Delta A_{1\text{ loop}} \simeq -\frac{5}{24}\sum_{q=d,s,b} V_{cq}^* V_{uq}\left(\frac{m_q}{M_W}\right)^2. \tag{31.2}$$

The CKM factors in the above equation have very different orders of magnitude

$$|V_{cd}^* V_{ud}| \simeq |V_{cs}^* V_{us}| \simeq 0.22 \qquad \text{and} \qquad |V_{cb}^* V_{ub}| \simeq (1.3 \pm 0.4) \times 10^{-4}. \tag{31.3}$$

Consequently, $|\Delta A_{1\ loop}| \sim 2 \times 10^{-7}$. The extraordinary smallness of this number is due to the tiny factors $(m_q/M_W)^2$ for the light quarks and to the small CKM angles in the b-quark contribution.

Since the important suppression factors are independent of gauge couplings, it is possible that higher orders in perturbation theory give dominant contributions to the radiative amplitude considered because they may not suffer the same dramatic suppression and are reduced only by powers of the gauge couplings.

With RGE, one can re-sum short distance QCD corrections in the leading logarithmic approximation which results in the effective Hamiltonian

$$H_{eff}(m_b > \mu > m_c) = \frac{4G_F}{\sqrt{2}}\sum_{q=d,s} V_{cq}^* V_{uq}[C_1(\mu)O_1^q + C_2(\mu)O_2^q + \sum_{i=3}^{8} C_i(\mu)O_i], \tag{31.4}$$

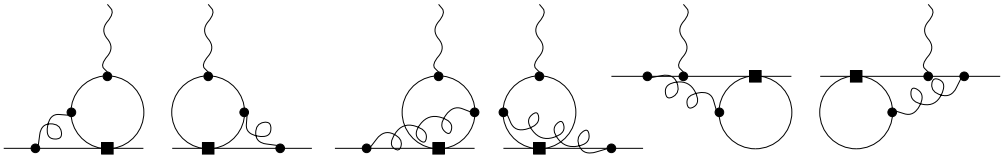

Figure 31.2: - Two-loop diagrams for the $c \to u\gamma$

where

$$O_1^q = (\bar{u}_\alpha \gamma_\mu P_L q_\beta)(\bar{q}_\alpha \gamma^\mu P_L c_\beta), \qquad q = d, s, b \tag{31.5}$$

$$O_2^q = (\bar{u}_\alpha \gamma_\mu P_L q_\alpha)(\bar{q}_\beta \gamma^\mu P_L c_\beta), \qquad q = d, s, b \tag{31.6}$$

$$O_7 = \frac{e}{16\pi^2}\, m_c (\bar{u}_\alpha \sigma_{\mu\nu} P_R c_\alpha) F^{\mu\nu}. \tag{31.7}$$

The Wilson co-efficiences C_i and remaining operators O_i are given explicitly in ref. [292].It is found that the leading logarithmic QCD correction will enhance the $c \to u\gamma$ by more than one order

$$|\Delta A_{LLA}| = [0.001 C_1(m_b) + 0.055 C_2(m_b)]\, |V_{cb}^* V_{ub}| = 0.060\, |V_{cb}^* V_{ub}| \simeq (8 \pm 3) \times 10^{-6}. \tag{31.8}$$

Moreover, including two loop contributions depicted by Fig.2, one finds the strength of $c \to u\gamma$ are further enhanced by more than two orders of magnitude

$$|A| = |V_{cs}^* V_{us}| \frac{\alpha(m_c)}{4\pi}\, (0.86 \pm 0.19) = (4.7 \pm 1.0) \times 10^{-3}. \tag{31.9}$$

After these surprising enhancements, in the SM the predicted branching ratio ($\mathcal{B}$) for $c \to u\gamma$ is found to be $\sim 10^{-8}$. However, even this is very small compared to the long distance contributions from s and u channel poles from nearby states and VMD contributions from ρ, ω, ϕ. These estimates suffer from uncertainties from several sources. The mass m_c is too large for the chiral symmetry approximation and it is too small for the HQET approximation. Hence, one has to resort to inspired guesswork [292, 293, 294]. In any case, the end results seem reasonable and agree with recent measurements. The $\mathcal{B}$ are in the range of 10^{-5} to 10^{-7}. The recent measurement of $\mathcal{B}(D^0 \to \phi^0\gamma) \sim 2.6 \times 10^{-5}$ by BELLE [295] is well within the expected range. However, it would be extremely hard to extract the small short distance contributions.

31.2.2 GIM Suppressed Decays

The short-distance component

Short-distance amplitudes are concerned with the QCD degrees of freedom (quarks, gluons) and any relevant additional fields (leptons, photons). Thus, the short distance part of the $D \to X_u \ell^+ \ell^-$ amplitude involves the quark process $c \to u\ell^+\ell^-$. It is usually most natural to employ an effective description in which the weak hamiltonian is expressed in

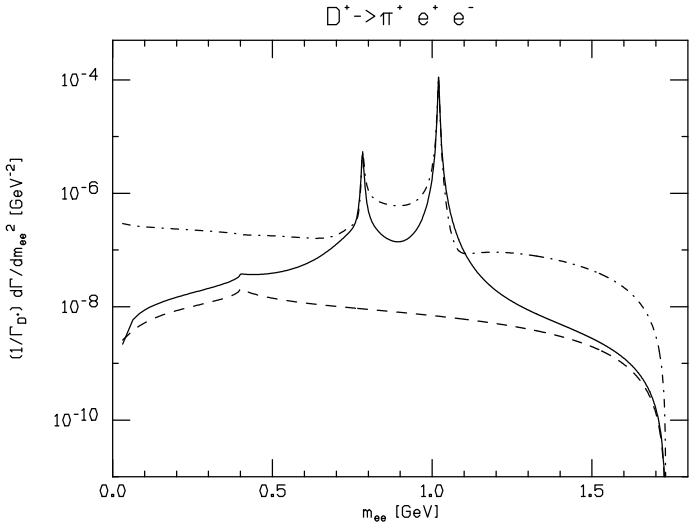

Figure 31.3: Dilepton mass distribution for $D^+ \to \pi^+ e^+ e^-$. The dashed (solid) line is the short-distance (total) SM contribution. The dot-dashed line is the R-parity violating contribution.

terms of local multiquark operators and Wilson coefficients. [297] For example, the effective hamiltonian for $c \to u\ell^+\ell^-$ with renormalization scale μ in the range $m_b \geq \mu \geq m_c$ is [2]

$$\mathcal{H}_{\rm eff}^{c\to u\ell^+\ell^-} = -\frac{4G_F}{\sqrt{2}}\left[\sum_{i=1}^{2}\left(\sum_{q=d,s} C_i^{(q)}(\mu)\mathcal{O}_i^{(q)}(\mu)\right) + \sum_{i=3}^{10} C_i'(\mu)\mathcal{O}_i'(\mu)\right] \quad . \tag{31.10}$$

In the above, $\mathcal{O}_{1,2}^{(q)}$ are four-quark current-current operators, $\mathcal{O}_{3-6}'$ are the QCD penguin operators, $\mathcal{O}_7$ ($\mathcal{O}_8$) is the electromagnetic (chromomagnetic) dipole operator and $\mathcal{O}_{9,10}$ explicitly couple quark and lepton currents. For example, we have

$$O_7' = \frac{e}{16\pi^2} m_c(\bar{u}_L\sigma_{\mu\nu}c_R)F^{\mu\nu} \ , \qquad O_9' = \frac{e^2}{16\pi^2}(\bar{u}_L\gamma_\mu c_L)(\bar{\ell}\gamma^\mu\ell) \quad . \tag{31.11}$$

The famous Inami-Lim functions [298] contribute to the Wilson coefficients C_{7-10} at scale $\mu = M_{\rm W}$.

Figure 31.3 displays the predicted dilepton mass spectrum for $D^+ \to \pi^+\ell^+\ell^-$. Several distinct kinds of contributions are included. The short-distance SM component corresponds to the dashed line, which is seen to lie beneath the other two curves. For reference, we cite the *inclusive* 'short distance' branching ratio,

$$\mathcal{B}r_{D^+\to X_u^+ e^+e^-}^{\rm (sd)} \simeq 2\times 10^{-8} \quad . \tag{31.12}$$

The long-distance component

The long-distance component to a transition amplitude is often cast in terms of hadronic entities rather than the underlying quark and gluonic degrees of freedom. For charm decays, the long-distance amplitudes are typically important but difficult to determine with

[2] Quantities with primes have had the explicit b-quark contributions integrated out

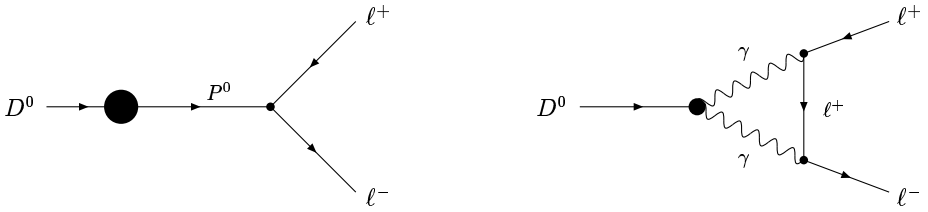

(a) (b)

Figure 31.4: Long distance contributions to $D^0 \to \ell^+\ell^-$.

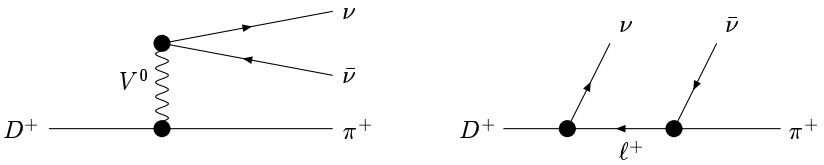

(a) (b)

Figure 31.5: Long distance contributions to $D^+ \to \pi^+\ell^+\ell^-$.

any rigor. There are generally several long-distance mechanisms for a given transition, *e.g.* as indicated for $D^0 \to \ell^+\ell^-$ in Fig.4 and for $D^+ \to \pi^+\bar{\nu}\nu$ in Fig.5.

Let us return to the case of $D^+ \to \pi^+\ell^+\ell^-$ depicted in Fig. 31.3. The solid curve represents the *total* SM signal, summed over both SD and LD contribution. In this case the LD component dominates, and from studying the dilepton mass distribution we can see what is happening. The peaks in the solid curve must correspond to intermediate resonances (ϕ, *etc*). The corresponding Feynman graph would be analogous to that in Fig.5(b) in which the final state neutrino pair is replaced by a charged lepton pair. One finds numerically that

$$\mathcal{B}r^{(\mathrm{SM})}_{D^+\to\pi^+e^+e^-} \simeq \mathcal{B}r^{(\ell\mathrm{d})}_{D^+\to\pi^+e^+e^-} \simeq 2\times 10^{-6} \quad . \tag{31.13}$$

The Standard Model Predictions

Basing the analysis in part on existing literature, [299] both SD and LD amplitudes for a number of FCNC D transitions have been calculated [291]. Results are collected in Table 31.1. As stated earlier, the current database for processes appearing in Table 31.1 consists entirely of upper bounds (or in the case of $D^0 \to \gamma\gamma$ no data entry at all). In all cases existing experimental bounds are much larger than the SM predictions, so there is no conflict between the two. For some (*e.g.* $D \to \pi\ell^+\ell^-$) the gap between SM theory and experiment is not so large and there is hope for detection in the near future. In others (*e.g.* $D^0 \to \ell^+\ell^-$) the gap is enormous, leaving ample opportunity for signals from New Physics to appear. This point is sometimes not fully appreciated and thus warrants some emphasis. It is why, for example, attempts to detect ΔM_{D} via D^0-$\bar{D}^0$ mixing experiments are so important.

Table 31.1: Standard Model predictions and current experimental limits for the branching fractions due to short and long distance contributions for various rare D meson decays.

Decay Mode	Experimental Limit	$\mathcal{B}r_{S.D.}$	$\mathcal{B}r_{L.D.}$
$D^+ \to X_u^+ e^+ e^-$		2×10^{-8}	
$D^+ \to \pi^+ e^+ e^-$	$< 4.5 \times 10^{-5}$		2×10^{-6}
$D^+ \to \pi^+ \mu^+ \mu^-$	$< 1.5 \times 10^{-5}$		1.9×10^{-6}
$D^+ \to \rho^+ e^+ e^-$	$< 1.0 \times 10^{-4}$		4.5×10^{-6}
$D^0 \to X_u^0 + e^+ e^-$		0.8×10^{-8}	
$D^0 \to \pi^0 e^+ e^-$	$< 6.6 \times 10^{-5}$		0.8×10^{-6}
$D^0 \to \rho^0 e^+ e^-$	$< 5.8 \times 10^{-4}$		1.8×10^{-6}
$D^0 \to \rho^0 \mu^+ \mu^-$	$< 2.3 \times 10^{-4}$		1.8×10^{-6}
$D^+ \to X_u^+ \nu \bar{\nu}$		1.2×10^{-15}	
$D^+ \to \pi^+ \nu \bar{\nu}$			5×10^{-16}
$D^0 \to \bar{K}^0 \nu \bar{\nu}$			2.4×10^{-16}
$D_s \to \pi^+ \nu \bar{\nu}$			8×10^{-15}
$D^0 \to \gamma\gamma$		4×10^{-10}	few $\times 10^{-8}$
$D^0 \to \mu^+ \mu^-$	$< 3.3 \times 10^{-6}$	1.3×10^{-19}	few $\times 10^{-13}$
$D^0 \to e^+ e^-$	$< 1.3 \times 10^{-5}$	$(2.3 - 4.7) \times 10^{-24}$	
$D^0 \to \mu^\pm e^\mp$	$< 8.1 \times 10^{-6}$	0	0
$D^+ \to \pi^+ \mu^\pm e^\mp$	$< 3.4 \times 10^{-5}$	0	0
$D^0 \to \rho^0 \mu^\pm e^\mp$	$< 4.9 \times 10^{-5}$	0	0

31.3 New Physics Analysis

There is a wide collection of possible New Physics models leading to FCNC D transitions. Among those considered in Ref.[291] are (i) Supersymmetry (SUSY): R-parity conserving, R-parity violating, (ii) Extra Degrees of Freedom: Higgs bosons, Gauge bosons, Fermions, Spatial dimensions, (iii) Strong Dynamics: Extended technicolor, Top-condensation.

We would restrict most of our attention to the case of supersymmetry. However, at the end a few remarks are made on the topic of large extra dimensions. The SUSY discussion divides naturally according to how the R-parity $R_{\rm P}$ is treated, where

$$R_{\rm P} \;=\; (-)^{3(B-L)+2S} \;=\; \left\{ \begin{array}{ll} +1 & \text{(particle)} \\ -1 & \text{(sparticle)} \end{array} \right. . \tag{31.14}$$

31.3.1 R-parity conserving SUSY

R-parity conserving SUSY will contribute to charm FCNC amplitudes via loops. To calculate R-parity conserving SUSY contributions, the so-called *mass insertion approximation* is always employed [300], which is oriented towards phenomenological studies and is also model independent. Let us first describe what is actually done and then provide a brief explanation of the underlying rationale.

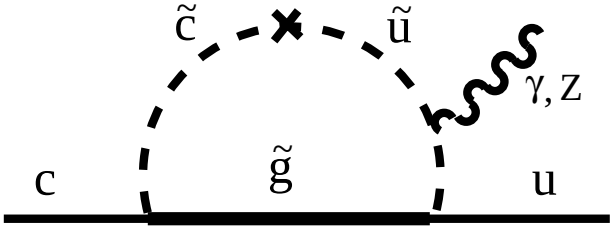

Figure 31.6: A typical contribution to $c \to u$ FCNC transitions in the MSSM. The cross denotes one mass insertion $(\delta^u_{12})_{\lambda\lambda'}$ and λ, λ' are helicity labels.

In this approach, a squark propagator becomes modified by a mass insertion (*e.g.* the '$\times$' in Fig.6 that changes the squark flavor [300, 301]. For convenience, one expands the squark propagator in powers of the dimensionless quantity $(\delta^u_{ij})_{\lambda\lambda'}$,

$$(\delta^u_{ij})_{\lambda\lambda'} = \frac{(M^u_{ij})^2_{\lambda\lambda'}}{M^2_{\tilde{q}}} \quad , \tag{31.15}$$

where $i \neq j$ are generation indices, λ, λ' denote the chirality, $(M^u_{ij})^2$ are the off-diagonal elements of the up-type squark mass matrix and $M_{\tilde{q}}$ represents the average squark mass. The exchange of squarks in loops thus leads to FCNC through diagrams such as the one in Fig.6. The role of experiment is to either detect the predicted (SUSY-induced) FCNC signal or to constrain the contributing $(\delta^u_{ij})_{\lambda\lambda'}$.

This topic is actually part of the super-CKM problem. If one works in a basis which diagonalizes the fermion mass matrices, then sfermion mass matrices (and thus sfermion propagators) will generally be nondiagonal. As a result, flavor changing processes can occur. One can use phenomenology to restrict these FCNC phenomena. The $Q = -1/3$ sector has yielded fairly strong constraints but thus far only D^0-$\bar{D}^0$ mixing has been used to limit the $Q = +2/3$ sector. In the analysis[291], charm FCNCs have been taken to be to be as large as allowed by the D-mixing upper bounds.

For the decays $D \to X_u \ell^+ \ell^-$ discussed earlier in Sect. 31.2.2, the gluino contributions will occur additively relative to those from the SM and so we can write for the Wilson coefficients,

$$C_i = C_i^{(\mathrm{SM})} + C_i^{\tilde{g}} \quad . \tag{31.16}$$

To get some feeling for dependence on the $(\delta^u_{12})_{\lambda\lambda'}$ parameters, we display the examples

$$C_7^{\tilde{g}} \;\propto\; (\delta^u_{12})_{\mathrm{LL}} \text{ and } (\delta^u_{12})_{\mathrm{LR}} \;, \qquad C_9^{\tilde{g}} \;\propto\; (\delta^u_{12})_{\mathrm{LL}} \quad , \tag{31.17}$$

whereas for quark helicities opposite [3] to those in the operators of Eq. (31.11), one finds

$$\hat{C}_7^{\tilde{g}} \;\propto\; (\delta^u_{12})_{\mathrm{RR}} \text{ and } (\delta^u_{12})_{\mathrm{LR}} \;, \qquad \hat{C}_9^{\tilde{g}} \;\propto\; (\delta^u_{12})_{\mathrm{RR}} \quad . \tag{31.18}$$

Moreover, the term in $\hat{C}_7^{\tilde{g}}$ which contains $(\delta^u_{12})_{\mathrm{LR}}$ experiences the enhancement factor $M_{\tilde{g}}/m_c$.

[3] We use the notation $\hat{C}$ for the associated Wilson coefficients.

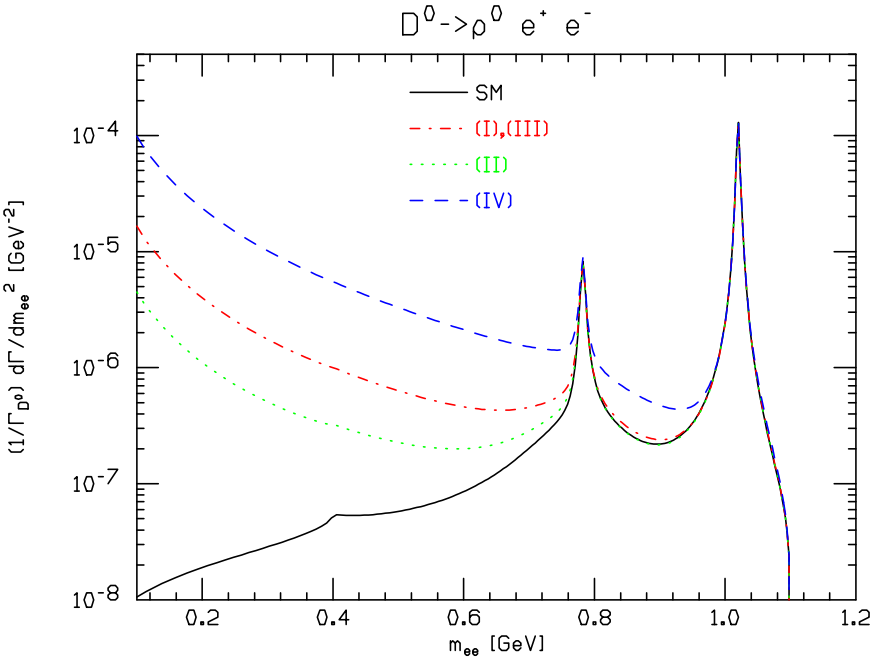

Figure 31.7: Dilepton mass distributions for $D^0 \to \rho^0 e^+ e^-$ in the mass insertion approximation of MSSM. The SM prediction (solid curve) is provided for reference and the MSSM curves refer to (i) $M_{\tilde{g}} = M_{\tilde{q}} = 250$ GeV, (ii) $M_{\tilde{g}} = 2M_{\tilde{q}} = 500$ GeV, (iii) $M_{\tilde{g}} = M_{\tilde{q}} = 1000$ GeV and (iv) $M_{\tilde{g}} = M_{\tilde{q}}/2 = 250$ GeV.

Numerically the effects in $c \to u\ell^+\ell^-$ are studied for the range of masses: (I) $M_{\tilde{g}} = M_{\tilde{q}} = 250$ GeV, (II) $M_{\tilde{g}} = 2\,M_{\tilde{q}} = 500$ GeV, (III) $M_{\tilde{g}} = M_{\tilde{q}} = 1000$ GeV and (IV) $M_{\tilde{g}} = (1/2)\,M_{\tilde{q}} = 250$ GeV. For some modes in $D \to X_u\ell^+\ell^-$, the effect of the squark-gluino contributions can be large relative to the SM component, both in the total branching ratio and for certain kinematic regions of the dilepton mass. The mode $D^0 \to \rho^0 e^+ e^-$ is given in Fig. 31.7. This figure should make clear the importance of measuring the low $m_{\ell^+\ell^-}$ part of the dilepton mass spectrum.

31.3.2 R-parity violating SUSY

The effect of assuming that R-parity can be violated is to allow additional interactions between particles and sparticles. Ignoring bilinear terms which are not relevant to our discussion of FCNC effects, we introduce the R-parity violating (RPV) super-potential of trilinear couplings,

$$\mathcal{W}_{\not R_p} = \epsilon_{ab}\left[\frac{1}{2}\lambda_{ijk}L_i^a L_j^b \bar{E}_k + \lambda'_{ijk}L_i^a Q_j^b \bar{D}_k + \frac{1}{2}\epsilon_{\alpha\beta\gamma}\lambda''_{ijk}\bar{U}_i^\alpha \bar{D}_j^\beta \bar{D}_k^\gamma\right] \quad , \tag{31.19}$$

where L, Q, $\bar{E}$, $\bar{U}$ and $\bar{D}$ are the standard chiral super-fields of the MSSM and i, j, k are generation indices. The quantities λ_{ijk}, λ'_{ijk} and λ''_{ijk} are *a priori* arbitrary couplings which total $9 + 27 + 9 = 45$ unknown parameters in the theory.

The presence of RPV means that *tree-level* amplitudes become possible in which a virtual sparticle propagates from one of the trilinear vertices in Eq. (31.19) to another.

In order to avoid significant FCNC signals (which would be in contradiction with current experimental limits), bounds must be placed on the (unknown) coupling parameters. As experimental probes become more sensitive, the bounds become ever tighter. In particular, the FCNC sector probed by charm decays involves the $\{\lambda'_{ijk}\}$. Introducing matrices $\mathcal{U}_{\rm L}$, $\mathcal{D}_{\rm R}$ to rotate left-handed up-quark fields and right-handed down-quark fields to the mass basis, we obtain for the relevant part of the superpotential

$$\mathcal{W}_{\lambda'} = \tilde{\lambda}'_{ijk}\left[-\tilde{e}^i_L \bar{d}^k_R u^j_L - \tilde{u}^j_L \bar{d}^k_R e^i_L - (\tilde{d}^k_R)^*(\bar{e^i_L})^c u^j_L + \ldots\right] \quad , \tag{31.20}$$

where neutrino interactions are not shown and we define

$$\tilde{\lambda}'_{ijk} \equiv \lambda'_{irs}\mathcal{U}^L_{rj}\mathcal{D}^{*R}_{sk} \quad . \tag{31.21}$$

Some bounds on the $\{\tilde{\lambda}'_{ijk}\}$ are already available from data on such diverse sources as charged-current universality, the ratio $\Gamma_{\pi\to e\nu_e}/\Gamma_{\pi\to\mu\nu_\mu}$, the semileptonic decay $D\to K\ell\nu_\ell$, *etc.* [303] The additional experimental implications of the preceding formalism are considered:

(i) For the decay $D^+ \to \pi^+e^+e^-$, the effect of RPV is displayed as the dot-dash line in Fig. 31.3. Here, the effect is proportional to $\tilde{\lambda}'_{11k}\cdot\tilde{\lambda}'_{12k}$ and we have employed existing limits on these couplings. Although the effect on the branching ratio is not large, but the dilepton spectrum away from resonance poles is seen to be sensitive to the RPV contributions. This case is not optimal because the current experimental limit on $\mathcal{B}r_{D^+\to\pi^+e^+e^-}$ is well above the dot-dash curve.

(ii) For $D^+ \to \pi^+\mu^+\mu^-$, the current experimental limit on $\mathcal{B}r_{D^+\to\pi^+\mu^+\mu^-}$ actually provides the new bound

$$\tilde{\lambda}'_{11k}\cdot\tilde{\lambda}'_{12k} \leq 0.004 \quad . \tag{31.22}$$

(iii) Another interesting mode is $D^0 \to \mu^+\mu^-$. Upon using the bound of Eq. (31.22) we obtain

$$\mathcal{B}r^{\not R_p}_{D^0\to\mu^+\mu^-} < 3.5\times10^{-6}\left(\frac{\tilde{\lambda}'_{12k}}{0.04}\right)^2\left(\frac{\tilde{\lambda}'_{11k}}{0.02}\right)^2 \quad . \tag{31.23}$$

A modest improvement in the existing limit on $\mathcal{B}r_{D^0\to\mu^+\mu^-}$ will yield a new bound on the product $\tilde{\lambda}'_{11k}\cdot\tilde{\lambda}'_{12k}$.

(iv) Lepton flavor violating processes are allowed by the RPV lagrangian. One example is the mode $D^0 \to e^+\mu^-$, for which existing parameter bounds predict

$$\mathcal{B}r^{\not R_p}_{D^0\to\mu^+e^-} < 0.5\times10^{-6}\times\left[\left(\frac{\tilde{\lambda}'_{11k}}{0.02}\right)\left(\frac{\tilde{\lambda}'_{22k}}{0.21}\right)+\left(\frac{\tilde{\lambda}'_{21k}}{0.06}\right)\left(\frac{\tilde{\lambda}'_{12k}}{0.04}\right)\right] \quad . \tag{31.24}$$

An order-of-magnitude improvement in $\mathcal{B}r^{\not R_p}_{D^0\to\mu^+e^-}$ will provide a new bound on the above combination of RPV couplings.

31.3.3 Large Extra Dimensions

For several years, the study of large extra dimensions ('large' means much greater than the Planck scale) has been an area of intense study. This approach might hold the solution

of the hierarchy problem while having verifiable consequences at the TeV scale or less. Regarding the subject of rare charm decays, one's reaction might be to ask *How could extra dimensions possibly affect the decays of ordinary hadrons?*. We provide a few examples in the following.

Suppose the spacetime of our world amounts to a $3+1$ brane which together with a manifold of additional dimensions (the bulk) is part of some higher-dimensional space. A field Θ which can propagate in a large extra dimension will exhibit a Kaluza-Klein (KK) tower of states $\{\Theta_n\}$, detection of which would signal existence of the extra dimension. Given our ignorance regarding properties of the bulk or of which fields are allowed to propagate in it, one naturally considers a variety of different models.

Assume, for example, the existence of an extra dimension of scale $1/R \sim 10^{-4}$ eV such that the gravitational field (denote it simply as G) alone can propagate in the extra dimension. [304] There are then bulk-graviton KK states $\{G_n\}$ which couple to matter. In principle there will be the FCNC transitions $c \to u\ G_n$ and since the $\{G_n\}$ remain undetected, there will be apparent missing energy. However this mechanism leads to too small a rate to be observable.

Another possibility which has been studied is that the scale of the extra dimension is $1/R \sim 1$ TeV and that SM gauge fields propagate in the bulk. [305] However, precision electroweak data constrain the mass of the first gauge KK excitation to be in excess of 4 TeV [306], and hence their contributions to rare decays are small [307].

More elaborate constructions, such as allowing fermion fields to propagate in the five-dimensional bulk of the Randall-Sundrum localized-gravity model [308], are currently being actively explored. [309]. Interesting issues remain and a good deal more study deserves to be done.

31.4 Summary

The FCNC charm decays are very rare in the SM due to the strong GIM suppression. In sharp contrast to $B \to X_s\gamma, K^*\gamma$, the SD contributions in radiative charm decays are much smaller than the LD contributions in the SM, which make the extraction SD contribution from future measurements of $D \to X_u\gamma$ and $D \to V\gamma$. Although, the LD contributions still dominate the rates, just as in the radiative decays, there are decays modes such as $D \to \pi\ell^+\ell^-$ and $D \to \rho\ell^+\ell^-$ where it is possible to access the SD physics away from the resonance contributions in the low di-lepton invariant mass region. As illustrated by Fig.3 and 7, for low di-lepton mass, the sum of long and short distance effects leaves a large window where the physics beyond the SM can be observed.

In summary, the FCNC modes are most sensitive to the effects of some new physics scenarios. If the sensitivity of experiment could reach below 10^{-6}, these new physics effects could be constrained highly. Such an experimental sensitivity, of course, make many radiative D decays accessible, however, may not illuminate short distance physics.

Past searches have set upper limits for the dielectron and dimuon decay modes [296]. In Table 31.2 and Table 31.3, the current limits and expected sensitivities at BES-III are summarized for D^+ and D^0, respectively. Detailed description on rare charm decays can be found in references [314, 315]. The charm meson radiative decays are also very

important to understand final state interaction which may enhance the decay rates. In Ref. [314, 315], the decay rates of $D \to V\gamma$ (V can be ϕ, ω, ρ and K^*) had been estimated to be $10^{-5} - 10^{-6}$, which can be reached at BES-III.

Mode	Reference Experiment	Best Upper limits(10^{-6})	BES-III ($\times 10^{-6}$)
$\pi^+e^+e^-$	CLEO-c [310]	7.4	0.03
$\pi^+\mu^+\mu^-$	FOCUS [311]	8.8	0.03
$\pi^+\mu^+e^-$	E791 [312]	34	0.03
$\pi^-e^+e^+$	CLEO-c [310]	3.6	0.03
$\pi^-\mu^+\mu^+$	FOCUS [311]	4.8	0.03
$\pi^-\mu^+e^+$	E791 [312]	50	0.03
$K^+e^+e^-$	CLEO-c [310]	6.2	0.03
$K^+\mu^+\mu^-$	FOCUS [311]	9.2	0.03
$K^+\mu^+e^-$	E791 [312]	68	0.03
$K^-e^+e^+$	CLEO-c [310]	4.5	0.03
$K^-\mu^+\mu^+$	FOCUS [311]	13	0.03
$K^-\mu^+e^+$	E687 [313]	130	0.03

Table 31.2: *Current and projected 90%-CL upper limits on rare D^+ decay modes at BES-III with 20 fb^{-1} data at $\psi(3770)$ peak. We assume the selection efficiencies for all modes are 35%.*

Mode	Reference Experiment	Best Upper limits(10^{-6})	BES-III ($\times 10^{-6}$)
$\gamma\gamma$	CLEO [316]	28	0.05
$\mu^+\mu^-$	D0 [318]	2.4	0.03
μ^+e^-	E791 [312]	8.1	0.03
e^+e^-	E791 [312]	6.2	0.03
$\pi^0\mu^+\mu^-$	E653 [319]	180	0.05
$\pi^0\mu^+e^+$	CLEO [317]	86	0.05
$\pi^0e^+e^-$	CLEO [317]	45	0.05
$K_S\mu^+\mu^-$	E653 [319]	260	0.1
$K_S\mu^+e^-$	CLEO [317]	100	0.1
$K_Se^+e^-$	CLEO [317]	110	0.1
$\eta\mu^+\mu^-$	CLEO [317]	530	0.1
$\eta\mu^+e^-$	CLEO [317]	100	0.1
ηe^+e^-	CLEO [317]	110	0.1

Table 31.3: *Current and projected 90%-CL upper limits on rare D^0 decay modes at BES-III with 20 fb^{-1} data at $\psi(3770)$ peak.*